range, from -174 ppm for cadmium nitrate to 13.7 ppm for the cadmium Tutton salt. It is interesting that the intermediate elements show the largest shift dispersion of 224 ppm (-154 to +70 ppm). Finally, in all tensors studied, the deshielded elements reflect dominant shielding contributions either from Cd-HO_2 bonds (solid marks) or from short Cd-O bonds (cross-hatched). The concomitant long-bond-shielding correlations are also evident.

Conclusion

The tensor-molecular reference frame orientation has been determined for six distinct ^{113}Cd shielding tensors. The tensor orientations corresponding to the cadmium calcium tetraacetate and cadmium maleate crystals were unambiguously determined by NMR and crystallographic data. A simple method for assigning symmetry-related tensors to the appropriate lattice sites was introduced and employed in the analysis of the cadmium acetate, formate, and diammonium disulfate crystals. Three tensor element-structure correlations have been clearly demonstrated. First, the least shielded tensor element is aligned nearly perpendicular to the plane containing water oxygens. Second, if the coordination sphere is devoid of water oxygens, then the deshielded element is oriented to maximize the short-bond oxygen shielding contribution. Third, the shielded tensor element is directed nearly perpendicular to the longest cadmium-oxygen bond. With single-crystal NMR data for nine distinct tensors in seven different crystals these orientational features appear to be general.

To final comments are required. First, all tensor configurations have been found to comply with the cadmium site symmetry. Hence, the potential for significant intermolecular shielding contributions must be noted. The single-crystal data reported here will provide the opportunity to evaluate the magnitude of the intermolecular shielding contributions to the ^{113}Cd nucleus. Second, as mentioned above, a motivation for this work is an understanding of the characteristic shielding of the resonances corresponding to Cd-substituted parvalbumin,[3] troponin C,[4] calmodulin,[5] insulin,[6] and concanavalin A.[7] The nitrate, suflate, and acetate crystals have shielding tensor elements in the biological range of -85 to -130 ppm (Figure 10). In each case the shielded elements reflect major contributions from long Cd-O bonds. Further, the only isotropic shift in this region corresponds to the 8-coordinate cadmium nitrate. Clearly, one would not expect nitrate ligands to be involved in the Cd-coordination sphere of substituted metalloproteins. However, these data do suggest the following. The isolated closed-shell Cd(II) ion is the most shielded species possible. Any perturbation of this configuration via bond formation results in a deshileding of the cadmium nucleus. Hence poor ligands, i.e., nitrate and sulfate, and long Cd-O bonds indicate weak bonding interactions and are readily understood to be a shielding influence. With this in mind, the nitrate shift may be a reflection of ligand type as much as the higher coordination number. Similarly, the inability to produce model compounds with ^{113}Cd chemical shifts in the biolobical region may reflect a preoccupation with coordination number at the expense of ligand type. Consequently, we are currently pursuing compounds with carbonyl and hydroxide oxygens as ligands.

Acknowledgment. The authors thank Professor C. A. Hare for kindly supplying the atomic coordinates for $CdCa(OAc)_4 \cdot 6H_2O$ and Professor R. G. Bryant for sharing the cadmium acetate data prior to publication. R.S.H. acknowledges Dr. L. Lebioda for many helpful discussions during the preparation of this work. Further, we are grateful to Professor E. L. Amma for providing access to the necessary diffraction equipment. This work was supported in part by the National Institutes of Health (Grant GM 26295) and profited from use of facilities at the University of South Carolina National Science Foundation Regional NMR Center (CHE 82-07445).

Registry No. ^{113}Cd, 14336-66-4; $CdCa(OAc)_4 \cdot 6H_2O$, 27923-94-0; $Cd(O_2CHCCHCO_2) \cdot 2H_2O$, 26266-36-4; $Cd(OAc)_2 \cdot 2H_2O$, 5743-04-4; $Cd(NH_4)_2(SO_4)2 \cdot 6H_2O$, 14767-05-6; $Cd_2(HCO_2)_4 \cdot 4H_2O$, 51006-62-3.

Macrocyclic Dioxo Pentaamines: Novel Ligands for 1:1 Ni(II)-O_2 Adduct Formation

Eiichi Kimura,*[1a] Ryosuke Machida,[1a] and Mutsuo Kodama[2b]

Contribution from the Department of Medicinal Chemistry, Hiroshima University School of Medicine, Kasumi, Minami-Ku, Hiroshima 734, Japan, and Department of Chemistry, College of General Education, Hirosaki University, Bunkyo, Hirosaki 036, Japan.
Received January 26, 1984

Abstract: Substituted and unsubstituted macrocyclic dioxo pentaamines, 1,4,7,10,13-pentaazacyclohexadecane-14,16-dione, form stable 1:1 square-pyramidal complexes with Ni(II) and Cu(II), which possess two deprotonated amide donors in equatorial positions. The high-spin Ni(II) complexes show a very low Ni(II,III) redox potential of +0.24 V vs. SCE and are easily oxidized chemically or electrochemically to Ni(III) complexes. Moreover, the Ni(II) complexes react with molecular oxygen to form 1:1 Ni(II)-O_2 adducts in aqueous solution, as established by a combination of polarographic, spectrophotometric, and manometric methods. Comparative studies with relevant pentadentate macrocyclic polyamine complexes revealed that the two deprotonated amide groups and the fifth amine donor incorporated in the 16-membered macrocyclic frame are essential for the formation of the Ni(II)-O_2 adducts. The oxygen uptake reaction is first order in $[O_2]$ and in $[NiH_{-2}L]^0$ in aqueous solutions, and the second-order rate constant is 1.7×10^2 s^{-1} M^{-1} at 35 °C. The attack of O_2 at the sixth coordinate site is competitively inhibited by imidazole. The O_2 complexation constant K_{O_2} is determined to be 1.9×10^4 M^{-1} at 35 °C by potentiometric titration. Novel features of the Ni(II)-O_2 adducts are discussed.

The dioxo tetraamines depicted in Figure 1 posess the novel ligand properties of both saturated macrocyclic tetraamines (N_4) and oligopeptides.[2-6] They can accommodate certain metal ions Cu^{2+}, Ni^{2+}, Co^{2+}, and Pd^{2+}, within the macrocyclic N_4 cavities with simultaneous dissociation of the two amide protons (like tripeptides) to afford 1:1 complexes generally designated as $[M^{II}H_{-2}L]^0$. Peptide complex features of the coordinated imide

(1) (a) Hiroshima University. (b) Hirosaki University.
(2) Kodama, M.; Kimura, E. *J. Chem. Soc., Dlaton Trans.* **1979**, 325.
(3) Kodama, M.; Kimura, E. *J. Chem. Soc., Dalton Trans.* **1979**, 1783.
(4) Ishizu, K.; Hirai, J.; Kodama, M.; Kimura, E. *Chem. Lett.* **1979**, 1045.
(5) Kodama, M.; Kimura, E. *J. Chem. Soc., Dalton Trans.* **1981**, 694.
(6) Machida, R.; Kimura, E.; Kodama, M. *Inorg. Chem.* **1983**, *22*, 2055.

0002-7863/84/1506-5497$01.50/0

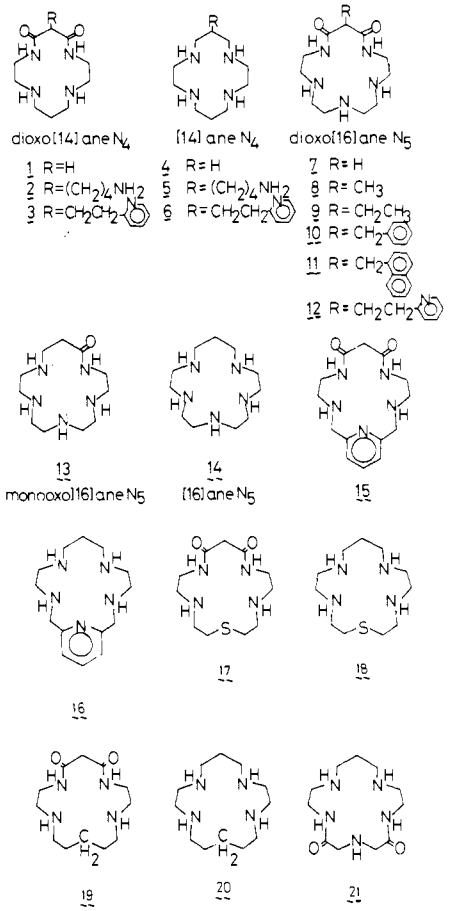

Figure 1. Macrocyclic polyamines used in the present investigation.

anions reinforce the coplanarity imposed by macrocyclic N_4 confinement.

The square-planar peptide complexes containing imide anions stabilize trivalent states of Cu[7] and Ni[8] and so do the doubly deprotonated macrocyclic dioxo tetraamine complexes.[5] A special advantage with the latter macrocyclic system is kinetic stabilization of the M(III) complexes. The former M(III) complexes decompose almost instantaneously. However, the redox potentials $E°$ for $M^{III,II}$ couples with macrocyclic dioxo N_4 complexes were not so low as to permit the generation of M(III) states by air oxidation.[5]

In our continuing efforts to devise simple macrocyclic ligands that produce proper ligand fields and steric environments so as to produce certain essential functions that occur in natural metal-containing enzymes,[9,10] we have been modifying these prototype ligand structures in various ways. In a recent communication[11] we reported the synthesis of 1,4,7,10,13-pentaazacyclohexadecane-14,16-dione (**7**, abbreviated as dioxo[16]aneN$_5$) and some properties of its Ni(II)–O_2 complexes. This compound has a fifth N donor within the macrocyclic frame (for its structure and those of all the following ligands, see Figure 1). The Ni(II) complex of dioxo pentaamine **7** showed an unexpectedly low $E°$ value of 0.24 V vs. SCE, while its Cu(II) complex exhibited an $E°$ value of 0.68 V, which is comparable to those for dioxo tetraamines such as **1**. The Ni(II) complex in aqueous solution turns brown on exposure to air in a similar fashion to the cases with electrochemical or chemical oxidation.[11] A detailed study astonished us in that the initial air-oxidized species were 1:1 Ni(II)–O_2 adducts. Previously molecular oxygen was shown to react with Cu(II)[12] and Ni(II) peptide complexes[13] to give Cu(III) and Ni(III) species as intermediates leading to the oxidation of the ligating peptides. There is a vast accumulation of reports on the formation of O_2 adducts with Fe(II), Co(II), Cu(I), Mn(II), Pt(0), Ir(0), or Ni(0) complexes,[14-18] but this is the first discovery of O_2 adducts with Ni(II). Even more surprisingly, the oxygen molecule bound to nickel(II) is apparently activated so as to oxygenate aromatic substrates to phenol products.[11] These findings prompted us to conduct thorough characterizations of Ni(II) complexes of macrocyclic pentaamines in order to spotlight the features of the Ni(II)–**7** system that make the observed 1:1 O_2 complexation and O_2 activation. For the present report, we have synthesized a broad family of macrocyclic pentaamines and the relevant homologues and investigated various properties of their Ni(II) complexes. We also present a full account of the unique oxygenation of Ni(II)–**7**.

Experimental Section

Instruments used in the present study were as follows: Hitachi R-40 (90 MHz) ^{1}H NMR spectrometer, JEOL JMS-01SG-2 mass spectrometer, JEOL JES-FE1X ESR spectrometer, Shimazu UV-200S UV–visible spectrophotometer, Shimazu GC-4CM gas chromatograph, Shimazu GCMS-7000 GC–mass spectrometer, and a Kyotodenshi AT-117 automatic titrator. Polarographic measurements were made with a manually operated apparatus described previously.[19,20]

Materials. Dioxo tetraamines **1** and **3**, tetraamines **4**, **6**, **18**, and **20**, and pentaamine **16** were prepared as before.[6,21] The purities of all thee macrocyclic ligands were checked by thin-layer chromatography and gas chromatography.[22] All of the new ligands were correctly analyzed for C, H, and N.

1,4,8,11-Tetraaza-13-(1-aminobutyl)cyclotetradecane-12,14-dione (2). 4-Bromobutyronitrile was treated with dimethyl malonate to prepare dimethyl (1-cyanopropyl)malonate.[23] The cyano group was reduced by $NaBH_4$–$CoCl_2$,[24] and the resulting dimethyl (1-aminobutyl)malonate was protected by carbobenzyloxy chloride (CBZ). The product was refluxed with equimolar 2,3,2-TET (1,4,8,11-tetraazaundecane) in dry methanol to get 1,4,8,11-tetraaza-13-(1-(carbobenzyloxyamino)butyl)cyclotetradecane-12,14-dione. The CBZ group was removed by HBr–CH_3COOH (48% aqueous HBr/Ch_3COOH = 1/1). The resulting 3HBr salt of **2** was converted to free base by Amberlite IRA-400: mp 197–198 °C; M^+ peak 299 (M_r = 299.41); ^{1}H NMR ($CDCl_3$–CD_3OD/Me_4Si) δ 1.20–1.90 (8 H, CCH_2C), 2.60–3.00 (10 H, NCH_2), 3.00–3.80 (5 H, $CONCH_2$ and $COCH_2CO$).

1,4,8,11-Tetraaza-13-(1-aminobutyl)cyclotetradecane (5). Dimethyl (1-cyanopropyl)malonate was refluxed with eqiumolar 2,3,2-TET in dry methanol to prepare 1,4,8,11-tetraaza-13-(1-aminopropyl)cyclotetradecane-12,14-dione, which was reduced with BH_3·THF (borane–tetrahydrofuran complx) to obtain **5**, which was purified as the 5HBr salt after recrystallization from C_2H_5OH–H_2O: mp 240 °C dec; M^+ peak 271 (M_r = 271.47); ^{1}H NMR (D_2O/Me_4Si) δ 1.48–1.75 (6 H, $CH_2CH_2CH_2$), 2.15–2.40 (2 H, CCH_2C), 2.96–3.25 (2 H, CH_2N), 3.25–6.63 (16 H, CH_2N).

1,4,7,10,13-Pentaazacyclohexadecane-14,16-dione (7) and Its Derivatives 8–12. The methanol solution of alkylated dimethyl malonate was refluxed with equimolar tetren (tetraethylenepentaamine) in methanol for 3 weeks. The products were separated by silica gel column chro-

(7) Bossu, F. P.; Chellapa, K. L.; Margerum, D. W. *J. Am. Chem. Soc.* **1977**, *99*, 2195.
(8) Bossu, F. P.; Margerum, D. W. *Inorg. Chem.* **1978**, *16*, 1210.
(9) Kimura, E.; Sakonaka, A.; Nakamoto, M. *Biochim. Biophys. Acta* **1981**, *678*, 172.
(10) Kimura, E.; Yatsunami, A.; Watanabe, A.; Machida, R.; Koike, T.; Fujioka, H.; Kuramoto, Y.; Sumomogi, M.; Kunimitsu, K.; Yamashita, A. *Biochim. Biophys. Acta* **1983**, *745*, 37.
(11) Kimura, E.; Sakonaka, A.; Machida, R.; Kodama, M. *J. Am. Chem. Soc.* **1982**, *104*, 4255.
(12) Burce, G. L.; Paniago, E. B.; Margerum, D. W. *J. Chem. Soc., Chem. Commun.* **1975**, 261.
(13) Bossu, F. P.; Paniago, E. B.; Margerum, D. W.; Kirksey, S. T., Jr.; Kurtz, J. L. *Inorg. Chem.* **1978**, *17*, 1034.
(14) Jones, R. D.; Summerville, D. A.; Basolo, F. *Chem. Rev.* **1979**, *79*, 139.
(15) McLendon, G.; Martell, A. E. *Coord. Chem. Rev.* **1976**, *19*, 1.
(16) Cheng, R. T.; Cook, C. D.; Nyburg, S. C.; Wan, W. Y. *Can. J. Chem.* **1971**, *49*, 3772.
(17) Otsuka, S.; Nakamura, A.; Tatsuno, Y. *J. Am. Chem. Soc.* **1969**, *91*, 6994.
(18) Dolphin, D., Ed. "The Porphyrins"; Academic Press: New York, 1978; Vol. V, pp 205–301.
(19) Kodama, M.; Kimura, E. *J. Chem. Soc., Dalton Trans.* **1976**, 116.
(20) Kodama, M.; Kimura, E. *J. Chem. Soc., Dalton Trans.* **1976**, 1720.
(21) Kimura, E.; Kodama, M.; Machida, R.; Ishizu, K. *Inorg. Chem.* **1982**, *21*, 595.
(22) Yatsunami, T.; Sakonaka, A.; Kimura, E. *Anal. Chem.* **1981**, *53*, 477.
(23) Gilman, H. et al., Eds. "Organic Syntheses"; Wiley: New York, 1956; Coll. Vol. I, p 250.
(24) Satoh, T.; Suzuki, S. *Tetrahedron Lett.* **1969**, *52*, 4555.

matography and purified by recrystallization from CH_3CN. Melting points of **7–12** are 179, 181, 203, 202, 218, and 207 °C, respectively. ^1H NMR and mass spectra (M^+) of these compounds support their structures.

1,4,7,10,13-Pentaazacyclohexadecan-14-one (13). The dry methanol solution of methyl acrylate (1 g in 10 mL of CH_3OH) was droped into a 30-mL methanol solution of tetren (1.5 g) at room temperature with stirring. The mixture was allowed to stir for 5 h at room temperature and then refluxed for 12 h. The product was separated by silica gel column chromatography and purified by recrystallization (from benzene). A 800-mg sample (yield 42%) of pure **13** was obtained: mp 143–145 °C; M^+ peak 243 (M_r = 243.35); ^1H NMR ($CDCl_3/Me_4Si$) δ 1.70 (s, 4 H, NH), 2.40 (t, 2 H, CH_2CON), 2.80 (s, 16 H, NCH_2), 3.45 (q, 2 H, $CONCH_2$), 8.10 (br s, 1 H, CONH).

3,6,10,13,19-Pentaazabicyclo[13.3.1]nonadeca-1,15,17-triene-7,9-dione (15). Dimethyl pyridine-2,6-dicarboxylate was reduced to the corresponding alcohol by $NaBH_4$ in methanol. The resulting 2,6-bis(hydroxymethyl)pyridine was converted to 2,6-bis(chloromethyl)pyridine with thionyl chloride in dry benzene, which was treated with ethylenediamine in ethanol solution. This product, 2,6-bis(1,4-diazapentyl)-pyridine was purified by distillation (bp 170 °C (3 mmHg)). The 200-mL methanol solution containing 1.2 g (5.4 mmol) of 2,6-bis(1,4-diazapentyl)pyridine and 800 mg (6 mmol) of dimethyl malonate was refluxed for 7 days. Upon evaporation white crystals precipitated from the solution. The crude product was purified by recrystallization (from benzene–CH_3OH). A 1.0-g sample (yield 64%) of pure **15** was obtained: mp 228 °C dec; M^+ peak 291 (M_r = 291.36); ^1H NMR ($CDCl_3$–CD_3OD/Me_4Si) δ 2.72–2.90 (4 H, $CONCH_2$), 3.20 (s, 2 H, $COCH_2CO$), 3.35–3.55 (8 H, NCH_2), 7.1 (d, 2 H, pyridine), 7.55 (t, 1 H, pyridine).

1,4,10,13-Tetraaza-7-thiocyclohexadecane-14,16-dione (17). The methanol solution (200 mL) of 2,2′-thiodiglycolic acid dimethyl ester (2 g, 11.2 mmol) and ethylenediamine (1.68 g, 28 mmol) was refluxed for 6 days. The products were separated by silica gel chromatography to isolate 780 mg (yield 30%) of 1,4,10,13-tetraaza-7-thiotridecane-5,9-dione, which was reduced with BH_3–THF to 1,4,10,13-tetraaza-7-thiodecane (220 mg) and purified by distillation (bp 180–200 °C (1 mmHg)). The linear thiotetraamine (220 mg, 1.08 mmol) was refluxed with 132 mg (1.00 mmol) of dimethyl malonate in 80 mL of methanol for 7 days, and the desired product **17** (100 mg, yield 36%) was separated by silica gel chromatography, followed by recrystallization (from benzene): mp 130–131 °C; M^+ peak 274 (M_r = 274.39); ^1H NMR ($CDCl_3$–CD_3OD/Me_4Si) δ 2.68–2.84 (12 H, NCH_2 and CH_2SCH_2), 3.35–3.55 (6 H, $CONCH_2$ and $COCH_2CO$).

1,4,10,13-Tetraazacyclohexadecane-14,16-dione (19). (*N*-Acetyl-*N*′-tosylethylenediamine)sodium salt (3.3 g, 12 mmol) was dissolved in 80 mL of dimethylformamide (DMF) to which 1.4 g (6 mmol) of 1,5-dibromopentane in 20 mL of DMF was added dropwise. The reaction mixture was heated at 80–90 °C for 24 h. After the solvent was evaporated, 100 mL of chloroform was added to the residue to precipitate NaBr, and the filtrate was evaporated to dryness under reduced pressure. The residue was refluxed in 100 mL of HBr–CH_3COOH (48% aqueous HBr (50 mL) + CH_3COOH (50 mL)) for 3 days. The acids were evaporated, and 50 mL of water was added to the residue. After the mixture was washed with 50 mL of chloroform, the water layer was concentrated until a white precipitate appeared. The precipitate was recrystallized from C_2H_5OH–H_2O to obtain 1.2 g (yield 19%) of pure 1,4,10,13-tetraazatridecane 4HBr salt, which was made free by Amberlite IRA-400. The methanol solution of the free base was refluxed for 7 days with equimolar dimethyl malonate. The product (500 mg) was separated by silica gel chromatography and recrystallized from CH_3CN: mp 132 °C; M^+ peak 256 (M_r = 256.34); ^1H NMR ($CDCl_3$–CD_3OD/Me_4Si) δ 1.38–1.60 (6 H, $CH_2CH_2CH_2$), 2.58–2.85 (8 H, NCH_2), 3.30–3.50 (6 H, $COCH_2CO$ and $CONCH_2$).

Potentiometric Measurements. The stock solution of nickel(II) was prepared from analytical grade $NiCl_2$ and standardized by titration with ethylenediaminetetraacetic acid (EDTA) by the method of Schwarzenbach.[25] The 1:1 complex formation constants $K_{NiH_{-i}L}$ for $Ni^{2+} + L \rightleftharpoons NiH_{-i}L + iH^+$ (1) and the oxygenation constant K_{O_2} for $NiH_{-2}L + O_2 \rightleftharpoons NiH_{-2}L{-}O_2$ (8) were determined by potentiometric titrations. Ligands in the presence of $HClO_4$ (1.0×10^{-3} M) were titrated with standard sodium hydroxide solution (0.1 N) in the presence of equimolar nickel(II), and the $-\log a_H$ (= pH) values were recorded 20 min after each increment of base. The titrations were performed under argon (passed through 1 N NaOH) for determination of $K_{NiH_{-i}L}$ and in air for K_{O_2}. All of the solutions were adusted to an ionic strength (I) of 0.2 M by addition of $NaClO_4$ and maintained at 15, 25, or 35 °C. The solubility of O_2 in water was taken from the literature:[26] 3.1, 2.6, and 2.2×10^{-4} M at 15, 25, and 35 °C, respectively. Every titration was repeated more than three times. The titration curves for (dioxo[16]aneN$_5$)Ni^{II} are shown in Figure 2, and all the $K_{NiH_{-2}L}$ values are summarized in Table I. The values of $-\log [H^+]$ were estimated from the pH reading: $-\log [H^+] = pH - 0.13$.

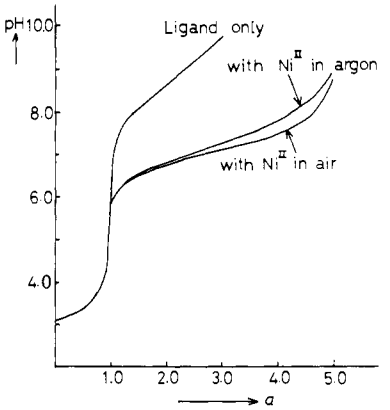

Figure 2. Potentiometric titration equilibrium curves of $7{\cdot}3HClO_4$ (10^{-3} M) in the presence of absence or equimolar Ni^{II} in argon and air atmosphere.

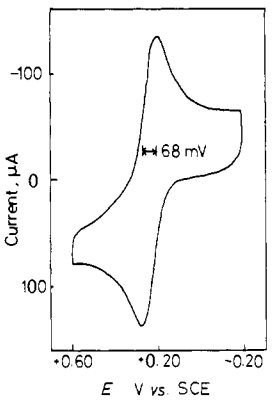

Figure 3. Cyclic voltammogram of $[NiH_{-2}L]^0$ (L = **7**, 2×10^{-3} M) in aqueous solution at a glassy carbon electrode: $E°$ = +0.24 V vs. SCE, ΔE = ±3 mV at pH 9.5 (nonbuffer), I = 0.5 M (Na_2SO_4), and scan rate = 2 mV/s.

Kinetic Measurements for O_2 Uptake. O_2 uptake rate was measured with a stopped-flow apparatus by observing an increase in absorbance at 320 nm at I = 0.2 M and 35 °C. The complex $[NiH_{-2}Li^7]^0$ was prepared in N_2 by mixing Ni(II) (5×10^{-4} M–4×10^{-3} M) with **7** (5–7% in excess) in borate buffer and allowing the mixture to equilibrate for 1 h. The concentration of $[NiH_{-2}L^7]^0$ used was always in large excess over that of O_2, and excellent pseudo-first-order kinetics were observed over 50% of the reaction. Typical rate data are shown in Table II.

Measurements of Magnetic Susceptibility. The magnetic susceptibilities of the Ni(II) complexes and the O_2 adducts were measured by Evans' method.[27] A 2% solution of *tert*-butyl alcohol in borate buffer (pH 9.4) was used as a reference. A 20 mM solution of a metal complex or an O_2 adduct in the same borate buffer was placed in an NMR tube (5-mm diameter). A capillary tube (2.5-mm diameter) in which the reference solution was loaded was immersed into the center of the NMR tube. Then, the ^1H NMR was measured at 35 °C, and the difference in chemical shift (for the methyl group of *tert*-butyl alcohol) caused by paramagnetic substances was read. The difference in chemical shifts (13 and 5.5 Hz correspond to 2.8 (S = 1) and 1.7 ($S = {}^1/_2$) μ_B, respectively) was determined by means of three measurements. Then, the magnetic susceptibilities were calculated according to Evans' equation.[27] The standard solution of aqueous Ni(II) exhibits 2.83 μ_B in the measurement. The results in terms of magnetic moment (±0.05 μ_B) are summarized in Table I.

Determination of $E°$ Values. Cyclic voltammetry was used to determine electrode potentials of Ni(II,III) couples for Ni(II) macrocyclic complexes.[5] Figure 3 shows a typical current–voltage response obtained

(25) Schwarzenbach, G. "Complexometric Titrations"; Interscience New York, 1957; p 82.

(26) "Chemical Handbook of Japan (Kagaku-binran)", Chemical Society of Japan; Maruzen: Tokoyo, Japan, 1973; p 571.

(27) Evans, D. F. *J. Chem. Soc.* **1959**, 2003.

Table I. Various Properties of Macrocyclic Polyamines and Their Ni(II) Complexes

ligand	mixed protonation const[a] log K_i	Ni(II) complex formula[a]	complexation const[a] $K_{NiH_{-2}L}$, M	magnetic susceptibility[b] μ_{eff}, μ_B	$Ni^{II,III}$ redox potential,[c] V vs. SCE
1	9.34, 5.42	$[NiH_{-2}L]^0$	$(7.1 \pm 1.0) \times 10^{-6}$	diamag	+0.81
2	10.17, 9.46, 5.75	$[NiH_{-2}L]^0$	$(7.1 \pm 1.0) \times 10^{-8}$	diamag	irrev
3	9.49, 5.80, 4.98	$[NiH_{-2}L]^0$	$(1.2 \pm 0.2) \times 10^{-6}$	diamag	+0.86
4	11.23, 10.30, 1.5, ~0.8	$[NiL]^{2+}$		1.8_8	+0.50
5	11.30, 10.94, 10.26, <2, <2	$[NiL]^{2+}$		1.9_9	+0.49
6	11.30, 10.10, 5.12, <2, <2	$[NiL]^{2+}$		1.4_8	+0.50
7	9.01, 8.69, <2	$[NiH_{-2}L]^0$	$(2.6 \pm 0.4) \times 10^{-9}$	2.8_1	+0.24
8	9.20, 8.07, <2	$[NiH_{-2}L]^0$	$(4.7 \pm 0.7) \times 10^{-10}$	2.8_2	+0.24
9	9.17, 8.00, <2	$[NiH_{-2}L]^0$	$(1.0 \pm 0.2) \times 10^{-10}$	2.8_4	+0.24
10	9.23, 7.91, <2	$[NiH_{-2}L]^0$	$(2.4 \pm 0.4) \times 10^{-11}$	2.8_1	+0.24
11	9.11, 7.82, <2	$[NiH_{-2}L]^0$	$(1.6 \pm 0.2) \times 10^{-11}$	unmeasureable[d]	+0.25
12	10.28, 8.75, 4.91	$[NiH_{-2}L]^0$	$(1.3 \pm 0.1) \times 10^{-8}$	2.8_8	+0.24
13	9.68, 8.65, 5.71, <2	$[NiH_{-1}L]^{1+}$	$(4.1 \pm 0.6) \times 10^{-5}$[e]	2.8_0	+0.46
14	10.42, 9.27, 7.06, <2, <2	$[NiL]^{2+}$		2.8_5	+0.66
15	9.34, 7.51	$[NiH_{-2}L]^0$	$(1.9 \pm 0.3) \times 10^{-13}$	2.8_2	+0.62
16	9.27, 8.35, 5.68, <2	$[NiL]^{2+}$		2.8_4	+0.53
17	8.28, 7.35, <2	$[NiH_{-2}L]^0$	$(2.6 \pm 0.4) \times 10^{-10}$	diamag	+0.41
18	9.33, 8.55, 4.49, ~3.2	$[NiL]^{2+}$		2.8_5	+0.77
19	10.42, 8.65	$[NiH_{-2}L]^0$	$(1.2 \pm 0.2) \times 10^{-11}$	diamag	irrev
20	9.93, 9.40, 5.54, ~3	$[NiL]^{2+}$		2.8_2	irrev
21	8.10, 4.61, ~2.4	$[NiH_{-2}L]^0$	$(2.2 \pm 0.2) \times 10^{-14}$	1.0_5	irrev

[a] At I = 0.2 M ($NaClO_4$) and 35 °C. Determined potentiometrically. [b] Measured in borate (0.05 M, pH 9.4) buffers (Ni^{II} complex concentration 10–20 mM) by Evans' method at 35 °C. [c] Determined by cyclic voltammetry at I = 0.5 M (Na_2SO_4), 25 °C and pH regions where Ni(II) is completely complexed. [d] The ligand is not soluble enough in water for the measurement of magnetic susceptibility. [e] Value for $K_{NiH_{-1}L}$ (= $[NiH_{-1}L][H^+]/[Ni][L]$).

Table II. Typical Kinetic Data for the Reaction of $[NiH_{-2}L^7]^0$ with O_2 at 35 °C and I = 0.2 M To Give an Oxygen Adduct

$[NiH_{-2}L^7]^0$, mM	$[O_2]$, mM	pH	[imidazole], mM	$10^{-2}k_{obsd}$, M^{-1} s^{-1}
4.00	0.115	9.07	0	1.70
2.00	0.115	9.07	0	1.65
1.00	0.115	9.07	0	1.74
0.50	0.115	9.07	0	1.81
1.00	0.058	9.07	0	1.62
1.00	0.029	9.07	0	1.69
1.00	0.115	8.57	0	1.78
1.00	0.115	9.07	0	1.74
1.00	0.115	9.54	0	1.69
1.00	0.115	10.04	0	1.71
1.00	0.115	10.00	0	1.70
1.00	0.115	10.00	32.9	1.41
1.00	0.115	10.00	64.8	1.19

for the nickel(II)–**7** complex (10^{-2} M) in Na_2SO_4 (0.5 M) solution at pH 9.6, 25 °C, and a scan rate of 100 mV/s. The initial solution contains only the divalent complex that generates the oxidation wave, while the oxidized trivalent complex formed in the anodic scan generates the reduction wave. This current–voltage response curve typifies almost all the nickel(II) complexes in this study. The separation of anodic and cathodic peaks, ΔE, was 70–90 mV, and peak height ratios were near unity. Slight variations (±3 mV) of peak potential separation with different scan rates (from 20 to 300 mV/s) were observed. Furthermore, both peak heights were proportional to the square root of the scan rate. These features are indicative of quasi-reversible (one-electron) electrochemical behavior, and therefore the midpoint between two peaks should be a reasonable estimate of $E°$ for the Ni(II,III) couples. In every case the midpoint was independent (within 3 mV) of the solution pH (8.0–10.5) and the concentrations of the complexes (5×10^{-1} to 4×10^{-3} M), the uncomplexing ligands (5×10^{-2} to 5×10^{-3} M), and the borate buffer (0.01–0.1 M). The electrode potentials $E°$ were obtained from an average of three measurements and have a reproducibility of ±3 mV, which are listed in Table I.

ESR Study. The ESR spectra of the O_2 adduct and O_2-free Ni(III) complex were carefully measured. A 1 mM solution of the Ni(II) complex was prepared by mixing benzyldioxo[16]aneN$_5$ (**10**) (in slight excess) and Ni(II) ion in aqueous solution (pH 9.5) under deaerated conditions. The O_2 adduct was obtained by air bubbling through the solution for 3 h. The O_2-free Ni(III) complex was prepared by anodic oxidation or $(NH_4)_2S_2O_8$ oxidation of the Ni(II) complex. The O_2 adduct or the Ni(III) complex solution was transferred to an ESR sample tube and immediately frozen in liquid nitrogen (77 K). X-Band ESR spectra were recorded (Figure 2 in ref 11) with the following: 100-kHz magnetic field modulation; microwave power, 1 mW; modulation, 5 G; field, 3100 ± 1000 G; sensitivity, × 500; response time, 0.3 s; recording speed, 4 min/360 mm. The g values were determined by taking the fourth signal of Mn(II) (g = 1.981) as standard, and the magnetic fields were calculated by the splitting of Mn(II) in MgO (ΔH = 86.9 G).

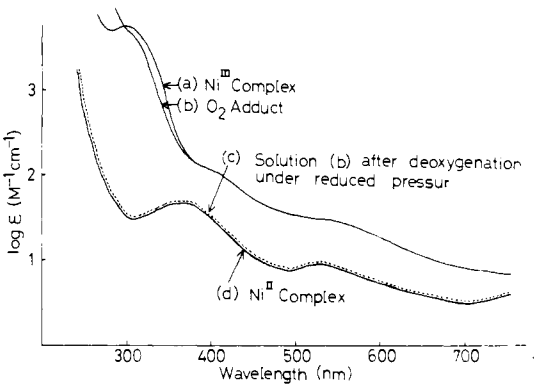

Figure 4. UV–visible spectra of benzyldioxo[16]aneN$_5$, **10**–Ni^{II} measured at 25 °C and pH 9.4: (a) $(NH_4)_2S_2O_8$ oxidized **10**–Ni^{II}, (b) O_2 adduct of **10**–Ni^{II}, (c) deoxygenated species of **10**–Ni^{II}, and (d) the starting **10**–Ni^{II}.

Results

Potentiometric Measurements of the Complex Formation Constants $K_{NiH_{-2}L}$ and the Oxygenation Constants K_{O_2}. Potentiometric titration curves of protonated dioxo ligands in the presence of equimolar Ni(II) or Cu(II) under argon exhibited the equilibrium positions to be at a lower pH than in their absence. The end point breaks all occurred at a = 5 except for **1**, **17**, and **19**, where they occurred at a = 4, indicating that all of the dioxo ligands form doubly deprotonated complexes $[MH_{-2}L]^0$. With monooxo ligand **13** and oxo-free ligands **4**–**6**, **14**, **16**, **18**, and **20**, $[NiH_{-1}L]^+$ and $[NiL]^{2+}$ are formed, respectively. The equilibrium constants $K_{NiH_{-2}L}$ were determined as follows. Complex formation (1) is competitive with ligand protonation (2) in the buffer region of the titration curve (Figure 2). The relationship of $K_{NiH_{-2}L}$ to

$$Ni^{2+} + L \rightleftharpoons NiH_{-2}L + 2H$$

$$K_{NiH_{-2}L} = \frac{[NiH_{-2}L][H^+]^2}{[Ni^{2+}][L]} \quad (1)$$

$$H_{i-1}L^{(i-1)+} + H^+ \rightleftharpoons H_iL^{i+}$$

$$K_i = \frac{[H_iL^{i+}]}{[H_{i-1}L^{(i-1)+}][H^+]} \quad (2)$$

K_i is given by eq 3 as shown previously[2,6] for dioxo tetraamines.

$$K_{NiH_{-2}L} = \frac{\{i(\alpha_H)_L - \beta_H\}\{\alpha(\alpha_H)_L - C_L\beta_H\}[H^+]^2}{(iC_L - \alpha)^2(\alpha_H)_L} \quad (3)$$

$i = 4$ for dioxo tetraamine[2,6] and $i = 5$ for dioxo pentaamine

$$(\alpha_H)_L = 1 + K_1[H^+] + K_1K_2[H^+]^2 + \cdots + K_1K_2 \cdots K_i[H^+]^i \quad (4)$$

$$\beta = i + (i-1)K_i[H^+] + \cdots + K_1K_2 \cdots K_{i-1}[H^+]^{i-1} \quad (5)$$

C = total ligand concentration

$$C = [NiH_{-2}L] + [L] + [HL^+] + \cdots + [H_iL^{i+}] \quad (6)$$

C = total concentration of Na^+ (from NaOH) and $[H^+]$

$$C = aC_L + [H^+] \quad (7)$$

Plots of the numerator vs. denominator of the right-hand side of eq 3 show linear lines passing through the origin for all the dioxo pentaamines. The constants $K_{NiH_{-2}L}$ are obtained from the gradient and summarized in Table I. We also obtained a $K_{CuH_{-2}L}$ value of 9.3×10^{-3} M for Cu(II)–**7**.

The titration curves of **7** and **8** with Ni(II) measured in air evidently differ from those measured in an argon atmosphere (see Figure 2), suggesting an interaction of the Ni(II) complexes of **7** and **8** with O_2. The oxygenation constants K_{O_2} defined by eq 8 were calculated by the graphic method previously described.[6]

$$Ni^{II}H_{-2}L + O_2 \rightleftharpoons Ni^{II}H_{-2}L\text{–}O_2$$

$$K_{O_2} = \frac{[Ni^{II}H_{-2}L\text{–}O_2]}{[Ni^{II}H_{-2}L][O_2]} \quad (8)$$

The results are $K_{O_2} = 1.9 \times 10^4$ M^{-1} for **7** and $K_{O_2} = 8.3 \times 10^3$ M^{-1} for **8** at 35 °C. In the case of **9–12**, the O_2 uptake rates were too slow to permit determination of their oxygenation constants by the potentiometric method. The complexes of **1–6** and **13–21** had no interaction with O_2.

The oxygenation constants K_{O_2} with **7** were determined at 35, 25, and 15 °C (1.9×10^4, 1.2×10^4, and 0.72×10^4 M^{-1}, respectively), and thermodynamic parameters ΔH (+8.5 kcal/mol) and ΔS (+47 eu) were obtained from van't Hoff plots.

O_2 Uptake Stoichiometry. The stoichiometry of O_2 uptake (by Ni(II)–**7**) was determined by polarographic measurement. The air-saturated control solution ($[O_2] = 2.7 \times 10^{-4}$ M) showed a polarographic wave height of 11.7 cm for the O_2 reduction. Mixing O_2 (2.03×10^{-4} M) with $Ni^{II}H_{-2}L$ (1.68×10^{-4} M) lowered the O_2 reduction wave height eventually to 1.40 cm ($= 3.2 \times 10^{-5}$ M). Hence, the $Ni^{II}H_{-2}L$ to a consumed O_2 ratio is 1:1.02. The 1:1 O_2 uptake was further confirmed as follows: When the reaction of O_2 (2.7×10^{-4} M) and $Ni^{II}H_{-2}L$ (2.5×10^{-4} M) at pH 9.0 and 25 °C was quenched after a few minutes, the $[O_2]$ consumed was 1.08×10^{-4} M and the $[Ni^{II}H_{-2}L\text{–}O_2]$ formed was 1.09×10^{-4} M, as calculated from an absorbance of 0.242 at 310 nm (complete aeration gave an absorbance of 0.550).

Reversible O_2 Uptake. The solution of $Ni^{II}H_{-2}L$ complex (L = **9** or **10**, 2×10^{-2} M in borate buffer at pH 9.4) was prepared by mixing a ligand (5–10% excess) and an equimolar Ni(II) ion under argon. After immediate measurement of the UV–visible spectrum (Figure 4d), the solution was exposd to air for 3 h at room temperature, during which time the Ni(II) complex was oxygenated and the solution turned from purple to dark yellow. After measurement of the UV spectrum of the O_2 adduct (Figure 4b), the solution was kept at 35 °C and placed under a reduced pressure of 15–20 mmHg with an aspirator, whereupon deoxygenation of the O_2 adduct occurred and was accompanied by a change in solution color back to purple. The UV–visible spectrum of the resulting solution (Figure 4c) was almost the same as that in Figure 4d. When the solution was exposed to air, oxygenation occurred again. This manipulation could be repeated several times. The deoxygenation was not observed with **7** or **8**. For **11** and **12**, the oxygenation appeared to be too slow to be followed.

Kinetics of O_2 Adduct Formation. The O_2 uptake rate was first order in both $[Ni^{II}H_{-2}L]^0$ and $[O_2]$. The values of the second-order rate constant k were independent of pH.

$$d[O_2 \text{ adduct}]/dt = k[NiH_{-2}L][O_2] \quad (9)$$

The addition of imidazole diminishes the O_2 uptake rate by an amount that is proportional to its concentration, implying competition between imidazole and O_2 for the sixth coordinate site of Ni(II), as expressed by eq 10 and 11. The observed rate should

$$Ni^{II}H_{-2}L + \text{imidazole} \xrightleftharpoons{K_{imid}} Ni^{II}H_{-2}L\text{–(imidazole)} \quad (10)$$

$$Ni^{II}H_{-2}L + O_2 \xrightarrow{k} Ni^{II}H_{-2}L\text{–}O_2 \quad (11)$$

be defined by eq 12, from which relation 13 is derived. The plots of k_{obsd}^{-1} against [imidazole] is linear. The equilibrium constant K_{imid} in eq 10 was determined from the gradient/intercept to be 6.6_7.

$$\text{rate} = k_{obsd}[NiH_{-2}L][O_2]$$

$$\text{rate} = k\frac{[NiH_{-2}L]}{[NiH_{-2}L] + [NiH_{-2}L\text{–(imidazole)}]}[NiH_{-2}L][O_2] \quad (12)$$

$$1/k_{obsd} = 1/k(1 + K_{imid}[\text{imidazole}]) \quad (13)$$

Magnetic Susceptibilities. The μ_{eff} values for compounds **7–16** weer all 2.8 μ_B ($S = 1$), which is consistent with a high-spin Ni(II) state, as is the pink color of the solutions and the typical visible absorption spectra. On the other hand, yellow Ni(II) complexes of macrocyclic dioxo tetraamines **1–3**, **17**, and **19** all proved to be diamagnetic. The oxo-free tetraamines 4, **5**, and **6** with or without side-arm donors exhibited intermediate values, indicating the existence of an equilibrium between the high-spin and the low-spin state. The Evans measurement firmly established μ_{eff} = 2.83 μ_B ($S = 1$) for the O_2 adduct $Ni^{II}H_{-2}L\text{–}O_2$ and 1.71 μ_B ($S = {}^1/_2$) for the Ni(III) complex $Ni^{III}H_{-2}L$ generated by $(NH_4)_2S_2O_4$ oxidation. The same techniques also found μ_{eff} of 1.7 μ_B for Cu(II)–**7** and ~0 for Cu(III)–**7**.

ESR Spectra. An ESR spectrum of the Ni(III) complex of **10** is shown in our previous communication.[11] The g values are 2.15 ($g_\perp$) and 2.02 ($g_\parallel$), indicating that the oxidation involves primarily nickel ion. If ligand oxidation had occurred, one would expect the values close to the spin-only value of 2.002.[28] The observed large orbital contribution to the paramagnetism suggests that the unpaired electron is located primarily on the metal ion, consistent with the formation of the trivalent nickel state.

The g values ($g_\perp > g_\parallel$) suggest a tetragonally distorted octahedral geometry for the low-spin d^7 Ni(III) complexes.[29,30] It is evident that one nitrogen donor atom ($I = 1$) coordinates to an axial position, since three lines of hyperfine splitting (22 G) occur in the $g_\parallel$ region.[31]

Discussion

Variation of Ni(II) Complexation Properties with Structural Parameters. The overall complexing behavior of the macrocyclic polyamine ligands is a composite function of the number and type of donor atoms, macrocyclic ring size, and charge type as well as the number and position of carbonyl substituents. With a broad family of macrocyclic ligands available, the observed Ni(II) complex geometries can be meaningfully related to Ni(II,III) redox potentials of these complexes.

The 14-membered tetraamines can contain Ni(II) in the center of the macrocyclic hole in a square-planar coordinate geometry.

(28) Barefield, E. K.; Mocella, M. T. *J. Am. Chem. Soc.* **1975**, *97*, 4238.
(29) Levecchio, F. V.; Gore, E. S.; Busch, D. H. *J. Am. Chem. Soc.* **1974**, *96*, 3109.
(30) Gore, E. S.; Busch, D. H. *Inorg. Chem.* **1973**, *12*, 1.
(31) Lappin, A. G.; Murray, C. K.; Margerum, D. W. *Inorg. Chem.* **1978**, *17*, 1630.

The rigid macrocyclic structure and especially the high ligand field of the deprotonated amide donors contribute to the stabilization of low-spin Ni(II) with dioxo ligand **1**. The 14-membered tetraamine **4**, without the two imide anions, gives a mixture of low-spin and high-spin Ni(II) complexes, as evidenced by the intermediate values of μ_{eff} (see Table I). Earlier spectroscopic measurements[32] showed the Ni(II)–**4** complex to be in low-spin

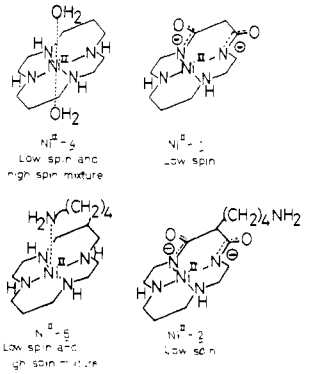

(71%) and high-spin (29%) equilibrium in aqueous solution at 25 °C. The strong coplanar effect of the dioxo group is also manifested by the fact that the low-spin state is retained even in the presence of a potential axial N donor on a side arm; see **2** and **3**.

The 16-membered dioxo pentaamine **7** having a larger cavity and five N donors would encircle the Ni(II) ion only in a square-pyramidal configuration with the two imide anion donors finding no place to stay other than the basal positions due to the steric requirement. The pink Ni(II)–**7** displays three d–d absorption bands with the low extinction coefficients (ϵ 1–10) characteristic of octahedral high-spin species (see Figure 4d), which is supported by the μ_{eff} value of 2.8 μ_B. If the two imide donors are in different positions as in **21**, the regular square-pyramidal geometry could hardly be attained and the result is a mixture of high- and low-spin complexes (see Table I). The monooxo[16]aneN$_5$ (**13**) and oxo-free [16]aneN$_5$ (**14**) offer similar square-pyramidal N$_5$ ligand environments to high-spin Ni(II) ions. The attachment of alkyl and aromatic substituents to **7** would not cause fundamental changes in the N$_5$ complex geometry, except for certain steric crowding effects, as indicated by generally smaller $K_{NiH_{-2}L}$ values for **8**–**11**. However, the pyridyl substituent in **12**,

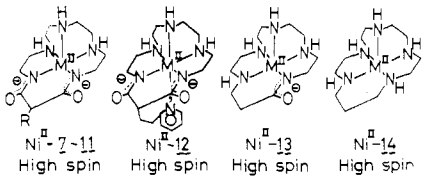

on the contrary, increases the complex stability by about a factor of 10. This fact, along with the failure of the Ni(II)–**12** complex to react with O_2 (see the following discussion), suggests the coordination of the pyridyl N at the sixth position. It is of some significance that the Ni(II) complexes of the N$_5$ ligands **7** and **14** are less stable than the corresponding N$_4$ homologues **1** and **4**, respectively, despite the fact that the former group offers one more donor atom than the latter. Evidently the better accommodation of the N$_4$ cavity to low-spin Ni(II) is of greater importance than the higher N$_5$ donor effect on high-spin Ni(II) so far as complex stability is concerned. Copper(II) also forms more stable complexes with the N$_4$ ligands than with the N$_5$ ligands.[33,34]

The location of the fifth N donor atom within and appendant to the macrocyclic frame is a critical factor governing the production of either high-spin or low-spin Ni(II) with dioxo pentaamines. Those having the fifth donor on a side arm (**2**, **3**) yield low-spin Ni(II) complexes, due to the strong tetragonal distortion effect of the macrocyclic dioxo N$_4$. In fact, these auxiliary fifth N donors do not assist in stabilizing the Ni(II) complexes, as shown by the $K_{NiH_{-2}L}$ values. On the other hand, when incorporated within the 16-membered macrocyclic frame **7**, the fifth N donor is constrained to an axial coordinate position by the macrocyclic structure. The axial amine of **7** and the axial pyridine N of **15**

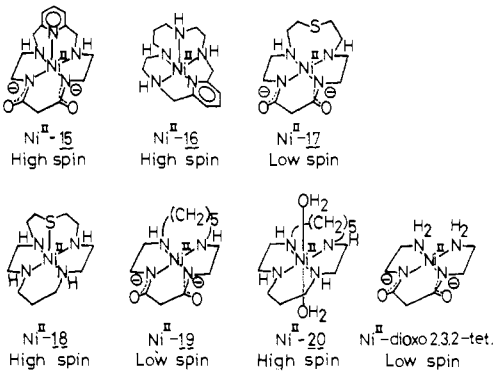

exert appreciable ligand field effect to raise the d_{z^2} orbital energy and yield the high-spin Ni(II) complexes, while the weaker σ donor of sulfur in **17** yields a low-spin Ni(II) complex. The axial coordination of the pyridine of **15** involves considerable strain, as a molecular model indicates. Thus, with the dioxo-free homologue **16**, the pyridine will stay at a basal position. Significant difference in visible absorptions, λ_{max} = 600 nm (ϵ 20) for **15** and 570 (shoulder) and 630 nm (ϵ 12) for **16**, supports this notion. When these donor atoms are substituted by carbon atom of **19**, the enclosed Ni(II) is low spin. Note that dioxo 2,3,2-tetraamine (= $(CH_2)_5$ bridge less **19**) yields a low-spin Ni(II) complex.[5] The strong ligand field effects of the imide anions are also demonstrated by the conversion of low-spin to high-spin Ni(II) upon removal of the dioxo functions; **17** vs. **18** and **19** vs. **20**.

Square-Pyramidal N$_5$ Coordinate Environments for Stability of Ni(III). The most remarkable discovery with the dioxo polyamine series is the dramatic drop of $E°$ values when the fifth donor atom is incorporated into the macrocyclic rings, from 0.81 V with **1** to 0.24 V with **7**, to 0.62 V with **15**, or to 0.41 V with **17**. This is a very distinctive feature, since in other ligand systems such as peptides (e.g., 0.71 V of Gly-Gly-His vs. 0.70 V of Gly–Gly–His–Gly)[8] and macrocylic tetraamines (e.g., 0.81 V of **1** vs. 0.86 V of **3**) $E°$ values are nearly insensitive to the additional axial coordination. Moreover, the $E°$ value of +0.24 V (vs. SCE) with **7** is exceptionally low among the reported Ni(II,III) redox values of the relevant polyamines[5,35,36] and oligopeptides in aqueous solutions.[7,8,13] Also, the fact that the Ni(II,III) potential (+0.24 V) is much smaller than the corresponding Cu(II,III) potential (+0.68 V)[11] with the same ligand has no precedent in the literature. The opposite trend is generally true with peptides[7,8] and macrocyclic tetraamines.[5,37] These facts, altogether, well illustrate how the square-pyramidal N$_5$ coordinate environments formed by **7** are extremely effective for the d^8 Ni(II) → d^7 Ni(III) transition.

Effect of Imide Anion Donors. The deprotonated peptide nitrogen is higher in the spectrochemical series and is a stronger σ donor than amine.[38] This is also true of the high-spin Ni(II)–macrocyclic pentaamine series, as qualitatively evidenced by the gradual shift of the d–d transition band ($^3A_{2g} \rightarrow {}^3T_{1g}$) of 510 (doubly deprotonated **7**), 520 (singly deprotonated **13**), and 527 nm (**14**, all ϵ 10 M^{-1} cm^{-1}). The stronger electron donor properties of the imide donors would be expected to help stabilize the higher

(32) Anichni, A.; Fabbrizzi, L.; Paoletti, P.; Clay, R. M. *Inorg. Chim. Acta* **1977**, *24*, L21.
(33) Kodama, M.; Kimura, E. *J. Chem. Soc., Dalton Trans.* **1978**, 1081.
(34) The Cu(II) complex of dioxo[16]aneN$_5$ is less stable ($K_{CuH_{-2}L}$ = 9.3 × 10^{-3}) than that of dioxocyclam (1.0 × 10^1).
(35) Fabbrizzi, L. *J. Chem. Soc., Chem. Commun.* **1979**, 1063.
(36) Zeigerson, E.; Ginzburg, G.; Schwartz, N.; Luz, Z.; Meyerstein, D. *J. Chem. Soc., Chem. Commun.* **1979**, 241.
(37) Kimura, E.; Koike, T.; Machida, R.; Nagai, R.; Kodama, M. *Inorg. Chem.*, in press.
(38) Billo, E. *Inorg. Nucl. Chem. Lett.* **1974**, *10*, 613.

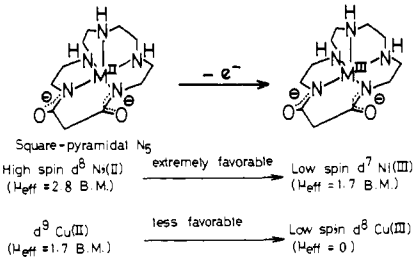

oxidation state of Ni, and this was found to be the case. $Ni^{II}H_{-2}L$ with **7** exhibits the lowest value (0.24 V), $Ni^{II}H_{-1}L$ with **13** (0.46 V) is intermediate, and $Ni^{II}L$ with **14** is the highest at 0.66 V. Each deprotonated amide group thus contributes to stabilization by 0.2 V in $E°$ values in macrocyclic pentaamine complexes. Such additivity is rare in linear peptide complexes of low-spin Ni(II).

The effect of imide donors on $E°$ is also observed in the sulfur-containing homologues, where the dioxo derivative **17** shows a lower $E°$ value of 0.41 V than the oxo-free **18** (0.77 V).

Effect of Axial Donors in the Macrocyclic Frame. The axial N donor atoms generally help to stabilize Ni(III). The relative ease of oxidation of Ni(II) to Ni(III) with amine **7** ($E°$ = 0.24 V) and thio ether **17** (0.41 V) may reflect the relative electron donor properties of N and S. The same order is seen for dioxo-free polyamines: amine **14** (0.66 V) vs. sulfur **16** (0.77 V). The greater $E°$ value of 0.62 V with pyridyl derivative **15** than those with amine **7** and sulfur **17** may be attributed to the negative effects of π back-bonding. The constrictive ring strain caused by the pyridyl bridging may work favorably for Ni(III)–**16**, accounting for the lower $E°$ value (0.53 V) than that for **14**.

It is of interest to note that the potential axial donors attached to the side arm in **2** and **3** do not stabilize the Ni(III) state like those incorporated in macrocycles. The strong square-planar constriction by the macrocyclic N_4 would cause tetragonal distortion so as to reduce the axial donor effects even on Ni(III). Our previous Ni(III) ESR spectral measurement indicated no axial bonding with **3**.[37]

After all these structural factors were taken into consideration, we have concluded that dioxo[16]aneN_5 (**7**) is the most appropriate ligand skeleton for stabilization of Ni(III). Thus, we were led to modify the basic structure of **7** and synthesize **8–12**. All of these complexes displayed almost the same $E°$ value of 0.24 V, indicating that the substituents have no major effect on the oxidation of Ni(II), as exhibited by the parent compound **7**.

Effect of Temperature and Solvation on $E°$ Value. Temperature has a minor influence on the $E°$ value of Ni(II)–**7** (0.245, 0.247, and 0.249 V at 15, 25, and 35 °C, respectively, with 0.1 M Na_2SO_4 and pH 10.3). The value of $(dE°/dT)$ = +0.18 is less than for Ni tetrapeptide complexes (+0.46 for tetraglycine),[39] supporting the notion that less solvation is needed for Ni(II,III)–N_5 coordinate **7** (eq 14) than for Ni(II,III)–N_4 coordinate tetrapeptide (eq 15).[39]

$$Ni^{II}H_{-2}L(H_2O) \rightleftarrows Ni^{III}H_{-2}L(H_2O) + e^- \quad (14)$$

$$Ni^{II}H_{-3}L + 2H_2O \rightleftarrows Ni^{III}H_{-3}L(H_2O)_2 + e^- \quad (15)$$

The $dE°/dT$ value for Ni(II,III)–macrocyclic N_4 (**4**) was 0.58 under the same conditions. The effect of solvation was further examined by measuring the $E°$ values as a function of solvent composition. As anticipated, increasing the 2-propanol content of the solvent, which lowers its solvating ability, increased the $E°$ values for the oxidation of Ni–**7**, 0.260 (2-propanol content 0%), 0.265 (27%), 0.270 (45%), and 0.272 V (75%) at 0.1 M $NaClO_4$, 25 °C, and pH 10.2. This upward trend is in contrast to the downward trend observed for Cu(II,III)–**1**: 0.693 (0%), 0.685 (22.5%), 0.678 (45%), and 0.672 V (75%). The latter process ($d^9 \rightarrow d^8$) should accompany desolvation (eq 16), and hence the

$$Cu^{II}H_{-2}L(H_2O)_2 \rightleftarrows Cu^{III}H_{-2}L + 2H_2O + e^- \quad (16)$$

decrease in the water content works favorably for this process.

(39) Youngblood, M. P.; Margerum, D. W. *Inorg. Chem.* **1980**, *19*, 3068.

It is interesting to note that in DMF, the Ni(II,III) potentials are extremely low, e.g., +0.02 V vs. SCE for Ni–**10** with 0.1 M $Bu_4N^+ClO_4^-$.

Nickel(III)–Dioxo[16]aneN_5 Complexes. A dark brown developed as the pink solution of Ni(II)–**7** with an initial unbuffered pH of 10.1 was oxidized electrochemically on a Pt wire at +0.50 V vs. SCE at room temperature. The oxidation was continued for 40 min to a final pH of 7.1. The oxidation product showed a UV–visible spectrum (λ_{max} 300 nm (ϵ 6900 M^{-1} cm^{-1}), see Figure 4a) similar to Ni(III) peptide complexes (e.g., 340 nm (e 4500) with Gly-Gly-Gly),[8] which constitutes evidence for Ni(III) complex formation. The ESR spectrum is consistent with the square-pyramidal N_5 coordination of low-spin d^7 Ni(III) at pH 7. The Ni(III) species is stable at pH less than 7 and remains for 4–5 h at room temperature, but it decomposes immediately at pH 10, as judged from the visible and ESR spectral changes. The Ni(III) species oxidizes KI, Fe(II), and ascorbic acid.

Interaction of O_2 with Ni(II)–Dioxo[16]aneN_5 Complexes. In view of the extremely low oxidation potential, we made an attempt to air oxidize Ni(II)–dioxo[16]aneN_5 complexes in aqueous solution. An intense brown color developed as in the electrochemical oxidation. (See the spectral change from d to b in Figure 4.) A further elaborate study established that the air oxidation products are the 1:1 ($Ni^{III}H_{-2}L$)–O_2 adducts. The supporting evidence for the novel 1:1 Ni(III)–O_2 complexes is as follows: (1) the $Ni^{II}H_{-2}L$ complex (where L = **7**) takes up an equimolar amount of O_2 in pH 9.5 borate buffer at 25 °C and I = 0.2 M (see Results); (2) the freshly oxygenated products show the intense band (assignable to CT from Ni to O_2) at λ_{max} 310 nm (ϵ 2200) for L = **7** and 290 nm (ϵ 4700) for **10** and possess oxidizing abilities such as oxidation of I^- and ascorbic acid similar to the electrochemically prepared Ni(III) species; (3) after several hours of exposure of Ni(II)–**7** to air in an unbuffered pH 9.8 aqueous solution at 25 °C, 0.5 mM $Ni^{III}H_{-2}L$–O_2 species (determined by the absorbance at 290 nm) was obtained [Its solution after deaeration with N_2 (to purge all of the free, uncomplexed O_2 in the solution) exhibited a new polarographic wave at $E_{1/2}$ = +0.17 V vs. SCE, which is ascribable to the reduction of the Ni-bound O_2]; (4) the electrochemical reduction of $NiH_{-2}L$–O_2 at potentials below its $E_{1/2}$ value proceeds to a quantitative recovery of the starting pink $Ni^{II}H_{-2}L$, as determined spectrometrically; (5) when the above deaerated 0.5 mM $Ni^{III}H_{-2}L$–O_2 solution is acidified to pH 3.0 by a few drops of acetic acid in an N_2 atmosphere, its wave height at $E_{1/2}$ = +0.17 V diminishes from 12 to 4.5 cm, indicating 63% [= (12 – 4.5)/12] decomposition of the oxygenated species. This wave decrease matches the emergence of a new wave (7.5 cm high) at −0.1 V vs. SCE, which is assigned to the reduction of free O_2, as separately confirmed [These polarographic observations are consistent with the spectrophotometric evidence of the diminished absorbance at 290 nm from 2.35 to 0.88 [(2.35–0.88)/2.35 = 63% decomposition]]; (6) the electrochemically generated $Ni^{III}H_{-2}L$ complexes do not release free O_2 at all when acidified with acetic acid; (7) the pH titration curve of Ni(II)–**7** in aerobic conditions fits the eq 8 derived for the formation of 1:1 O_2 adducts. For the 1:1 O_2 adduct, we propose structure I where O_2 occupies the sixth coordinate site.[40]

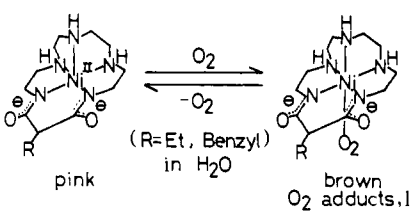

It is of interest to note that the reactivity of Ni(II)–**7–12** toward O_2 greatly varies with R substituents, although they show the same Ni(II,III) redox potentials. The release of O_2 from the O_2 adduct

(40) Determination of the O_2 stretching frequency is certainly needed. However, IR and Raman spectroscopic measurements of the Ni^{II}–**7**–O_2 adduct have not been successful so far.

under reduced pressure does not occur for unsubstituted **7** and methyl-substituted **8**, while it occurs for ethyl-substituted **9** or benzyl-substituted **10**. This suggests that steric effects are responsible for the shift of the O_2 uptake equilibrium. The complex Ni(II)–**11**, having a bulkier naphthylmethyl substituent, shows no reaction with oxygen even after a few days of exposure. A similar inertness of Ni(II)–**12** to O_2 is attributed to the occupancy of the sixth coordinate site by the pyridyl N.

The reaction of $Ni^{II}H_{-2}L$ (where L = **7**) with O_2 in aqueous solution follows second-order kinetics: rate = $k[Ni^{II}H_{-2}L][O_2]$ where $k = 1.7 \times 10^{-2}$ M^{-1} s^{-1} at 35 °C. A similar rate law holds for oxygen uptake of Co(II)–**14**[41] ($k = 2.2 \times 10^5$ M^{-1} s^{-1} at 25 °C) and Fe(II)–**16** ($k = 1.4 \times 10^2$ M^{-1} s^{-1} at 25 °C and pH 8.0).[21] All these reactions involve the same process of replacement of coordinate water by O_2. The site for O_2 coordination was shown to be competitively occupied by imidazole. Molecular oxygen was previously shown to react with Ni(II) tetrapeptide complexes (e.g., with tetraglycine $E° = 0.54$ V vs. SCE) in aqueous solution.[13] However, it is an autocatalytic process in which small amounts of the initially formed Ni(III) species catalyze the peptide oxidation. The O_2 uptake kinetics are expressed in a more complex form.

Properties of the Ni(III)–O_2 Adducts. The magnetic susceptibility of 2.83 μ_B of the starting, pink Ni(II)–**10** complex remains unchanged upon oxygenation to the brown 1:1 O_2 adduct, while it becomes 1.71 μ_B upon electrochemical or chemical oxidation to the brown Ni(III)–**10** complex. The paramagnetic properties of the 1:1 O_2 adduct with two unpaired electrons ($S = 1$) may be interpreted in terms of weak interaction of Ni(III) with the superoxide ion O_2^- where the spin coupling is weak.[40] The localized Ni(III) character is well demonstrated by the fact that the UV spectra of the Ni(III)–O_2 adducts are similar to those of the electrochemically generated Ni(III) complexes. The fresh O_2 adduct of Ni(II)–**10** exhibits an ESR spectrum very similar to the one obtained for Ni(III) species (Figure 2 in ref 11), although the intensity of the former is weaker about by a factor of $^1/_{20}$. A objection may be raised that the ESR spectrum of the O_2 adduct is more like that of an autoxidized Ni(III) contaminant. However, we observed that this ESR signal almost completely disappears upon deoxygenation in vacuo. Upon reoxygenation we obtained almost the same spectrum as the first one. For further evidence of the Ni(III)–O_2 adducts, the ESR spectrum of the oxygenated species with **10** prepared in $^{17}O_2$ was measured, which exhibits (ill-defined) three new lines ($J = 8.4$ G) in the $g_{\parallel}$ region where there is another set of three strong lines of the superhyperfine splitting (due to ^{14}N–Ni(III) coupling, $J = 22$ G). Although the detailed discussion awaits a more elaborate ESR study, this new splitting may be interpreted to be the result of a weak interaction of Ni(III) with the nuclear spin of $^{17}O_2$ ($I = {}^5/_2$). The Ni(III) spectrum of the $^{16}O_2$ ($I = 0$) adduct does not show such splitting.

Novel Features of the Ni(II)–O_2 Complexes. Since Ni(II) has never been considered to be a likely candidate for O_2 uptake, the manner in which O_2 is bound to the Ni(II)–dioxo[16]aneN$_5$ complexes is a matter of great interest. The situation could be compared with Fe(II)- and Co(II)–macrocyclic polyamine systems.[4,6,21,41,42] Addition of O_2 to these metal complexes is considered to involve a formal oxidation of the metal center with a concomitant reduction of the coordinated O_2. Thus, the coordinated dioxygen can be viewed as more or less resembling a coordinated superoxide anion, O_2^-. In comparing the oxygenation of Ni(II), Fe(II), and Co(II) systems, the direct oxidation of M(II)–macrocyclic polyamines by O_2 (eq 17 and 18) may be first

$$O_2 + e^- \rightarrow O_2^- \quad E° = -0.33 \text{ V vs. NHE}^{43} \qquad (17)$$

$$M^{II}\text{–macrocyclic polyamine} \rightarrow M^{III}\text{–macrocyclic polyamine} \qquad (18)$$

postulated. It has been established that all of these M(II) complexes form O_2 adducts in aqueous solutions.[4,6,21,41,42] If we write an isolated equilibrium (eq 19) using the half-reaction in eq 17 to oxidize Ni^{II}–**7** ($E° = +0.49$ V vs. NHE), we obtain

$$Ni^{II}\text{–}\mathbf{7} + O_2 \rightleftharpoons Ni^{III}\text{–}\mathbf{7} + O_2^- \qquad (19)$$

$$E° = -0.82 \text{ V}$$

$$K_{eq} = \frac{[Ni^{III}\text{–}\mathbf{7}][O_2^-]}{[Ni^{II}\text{–}\mathbf{7}][O_2]} = 10^{-14}$$

In other words, O_2, as an uncomplexed species, is thermodynamically incapable of oxidizing Ni^{II} to Ni^{III} to any practical extent. The energetics ought to be greatly improved on O_2 coordination to Ni. By comparison, such an electron-transfer process is more feasible for Fe(II) and Co(II). The $E°$ values for oxidation of Fe(II) to Fe(III) and of Co(II) to Co(III) are less negative than for the oxidation of Ni(II) shown in eq 19. Under the same conditions as were maintained for the oxidation of Ni(II) we found $E°$ values (vs. NHE) for eq 18 as follows: −0.02 V for Fe(II)–**16**,[21] −0.05 V for Co(II)–**14**, and −0.06 V for Co(II)–**1**. These values were determined polarographically. This fact implies that oxygenation of Co(II) and Fe(II) complexes could be described more as an oxidative addition type interaction and also that further electron transfer to distinct M(III) and O_2^- species is more likely for Co and Fe than for Ni.

Since an electron-transfer reaction is least likely, the question arises how the ionic type of bonding $M^{III}\cdots O_2^-$ can be adopted with Ni. Although the ionic bond strength is unknown, the polar solvation effects of water would undoubtedly provide a driving force for the reaction of the neutral $[Ni^{II}H_{-2}L]^0$ species with neutral O_2 to yield the dipolar $[Ni^{III}H_{-2}L]^+\cdots O_2^-$ products. In Co(II)–Schiff bases complexes, O_2 affinity appreciably increases in polar solvents,[44] which is ascribed to the stabilization of the polar Co(III)–O_2^- species in more polar solvents. We have found anomalous higher O_2 affinity at higher temperature with Ni(II), which implies a positive contribution to the entropy change upon oxygen binding to the Ni(II) complexes in aqueous solvents. This unusual behavior may lend a support to the above argument concerning the dipolar structure of the oxygenated product in aqueous solutions. The novel chemical reactivity of the Ni-bound O_2 that can attack benzene to yield phenol[11] may also be accounted for by the dipolar structure.

The fact that the Ni(II)–dioxo[16]aneN$_5$ with the sixth coordinate site being occupied, as in Ni(II)–**12**, is unreactive with O_2, despite the identical $E°$ value of 0.24 V, suggests an inner-sphere electron-transfer process for the formation of Ni(III)$\cdots O_2^-$. The prior Ni–O_2 bond formation would be facilitated by the interaction of high-spin Ni(II) with the triplet ground-state O_2. This situation bears a resemblance to biological heme O_2 uptake where high-spin Fe(II) interacts with triplet O_2,[45] although the resulting Fe–O_2 adducts are diamagnetic. The importance of the high-spin state of Ni(II) for O_2 uptake may also be illustrated by the fact that dianionic macrocyclic tetraamine complexes with low-spin Ni(II) were not reported to be subject to oxygenation despite possessing much lower (or even negative) $E°$ values than our +0.24 V for Ni(II,III) couples.[46]

Conclusions

16-Membered macrocyclic dioxo pentaamines are unique ligands that enable high-spin Ni(II) to interact with molecular oxygen to yield 1:1 O_2 adducts. The essential features of the (dioxo pentaamine)nickel (II) complexes are the inclusion of an axial N donor within the macrocyclic frame and the generation of two imide anions upon interaction with high-spin Ni(II). The effect of this complexation is to lower the Ni(II,III) redox potential to +0.24 V vs. SCE, the lowest value ever reported for high-spin Ni(II) ⇌ Ni(III) couples. This $E°$ value is just suitable, neither too high nor too low, for stabilization of Ni^{II}–O_2 bonding in

(41) Kodama, M.; Kimura, E. *Inorg. Chem.* **1980**, *19*, 1871.
(42) Kodama, M.; Kimura, E. *J. Chem. Soc., Dalton Trans.* **1980**, 327.
(43) Wood, P. M. *FEBS Lett.* **1974**, *44*, 22.
(44) Carter, M. J.; Rillema, P. P.; Basolo, F. *J. Am. Chem. Soc.* **1974**, *96*, 392.
(45) Bolton, W.; Perutz, M. F. *Nature (London)* **1970**, *228*, 551 and 726.
(46) Pillsburg, D. G.; Busch, D. H. *J. Am. Chem. Soc.* **1976**, *98*, 7836.

aqueous solution that is better represented by $Ni^{III}\cdots O_2^-$ dipolar formalism. The interaction of high-spin Ni(II) with triplet O_2 resembles the biological O_2 uptake system of heme-containing high-spin Fe(II), although the resulting 1:1 O_2 adducts are paramagnetic ($S = 1$) with Ni and diamagnetic with heme. Attaching an ethyl or benzyl substituent to the macrocycle ring enhances the reversibility of the O_2 adduct formation. That metal-bound superoxide is a reactive oxygen species is a hypothesis of long standing.[47] The present Ni^{III}–O_2^- serves as an appropriate example, since the Ni-bound O_2 is activated to the degree that it can attack benzene to yield phenol.[48] We believe a new O_2 chemistry will evolve out of the macrocyclic polyamine complexes of high-spin Ni(II).

(47) Michelson, A. M.; McCord, J. M.; Fridovich, I. "Superoxide and Superoxide Dismutases"; Academic Press: London, 1977; p 77.
(48) We have recently proved that the phenol oxygen is entirely and directly derived from O_2: Kimura, E.; Machida, R. *J. Chem. Soc., Chem. Commun.* **1984**, 499.

Registry No. 2, 91327-96-7; **5**, 63972-28-1; **5**·5HBr, 91328-06-2; **7**, 76201-28-0; **8**, 91327-97-8; **9**, 91327-98-9; **10**, 91327-99-0; **11**, 91328-00-6; **12**, 91328-01-7; **13**, 91328-02-8; **15**, 91328-03-9; **17**, 91328-04-0; **19**, 91328-05-1; Ni^{II}-**1**, 78737-53-8; Ni^{II}-**2**, 91328-07-3; Ni^{II}-**3**, 91384-59-7; Ni^{II}-**4**, 64616-26-8; Ni^{II}-**5**, 91328-08-4; Ni^{II}-**6**, 91328-09-5; Ni^{II}-**7**, 80400-19-7; Ni^{II}-**8**, 91328-10-8; Ni^{II}-**9**, 91328-11-9; Ni^{II}-**10**, 80389-72-6; Ni^{II}-**11**, 80389-73-7; Ni^{II}-**12**, 91328-12-0; Ni^{II}-**13**, 91328-13-1; Ni^{II}-**14**, 77321-28-9; Ni^{II}-**15**, 91328-14-2; Ni^{II}-**16**, 91328-15-3; Ni^{II}-**17**, 91328-16-4; Ni^{II}-**18**, 90751-78-3; Ni^{II}-**19**, 91328-17-5; Ni^{II}-**20**, 91328-18-6; Ni^{II}-**21**, 91328-19-7; Ni^{III}-**10**, 82135-48-6; Cu^{II}-**7**, 80386-21-6; Cu^{III}-**7**, 91328-20-0; 13-(4-(carbobenzyloxyamino)butyl)-1,4,8,11-tetraazacyclotetradecane-12,14-dione, 91327-94-5; 13-(3-cyanopropyl)-1,4,8,11-tetraazacyclotetradecane-12,14-dione, 63972-23-6; 1,4,10,13-tetraaza-7-thiotridecane-5,9-dione, 91327-95-6; 1,4,10,13-tetraaza-7-thiotridecane, 80042-28-0; 1,4,10,13-tetraazatridecane, 35513-91-8; imidazole, 288-32-4.

Mechanism of Acetylene and Olefin Insertion into Palladium–Carbon σ Bonds

Edward G. Samsel and Jack R. Norton*

Contribution from the Department of Chemistry, Colorado State University, Fort Collins, Colorado 80523. *Received January 10, 1984*

Abstract: The intramolecular acetylene insertion reactions of $ClL_2PdCO_2(CH_2)_nC{\equiv}CCH_3$ (**1a**, L = Ph_3P, $n = 2$; **1b**, L = p-tol_3P, $n = 2$; **2**, L = Ph_3P, $n = 3$) and the intramolecular olefin insertion reaction of $ClL_2PdCO_2CH_2CH_2CH{=}CH_2$ (**3**, L = Ph_3P) have been investigated. The acetylene insertion reactions give stable vinyl complexes **5a**, **5b**, and **6**; the olefin insertion reaction gives an unsaturated lactone by β-hydrogen elimination from the initially formed insertion product. Kinetic and ^{31}P NMR studies show that, as predicted by Thorn and Hoffmann, the reactions proceed by a four-coordinate mechanism, with the triple or double bond displacing a phosphine ligand in a rapidly maintained equilibrium prior to insertion. the triple bond in **2**, with the longer carbon chain, is more easily coordinated than that in **1a** but inserts less rapidly after coordination.

The insertion of carbon–carbon multiple bonds into metal–carbon bonds has traditionally been assumed to be a key step in many important reactions in homogeneous catalysis. For example, the catalytic trimerization[1,2] and (in some cases) the carboalkoxylation[3] of acetylenes are believed to involve the insertion of triple bonds into metal–carbon σ bonds; the catalytic arylation,[4] oligomerization,[5] and (again, in some cases) carboalkoxylation[3] of olefins have been said to involve the insertion of double bonds into metal–carbon σ bonds. In view of the importance of these catalytic reactions and of the fact that alternative mechanisms not involving insertion have recently been put forward for some of them (e.g., for ethylene and propylene polymerization[6]), considerable effort has been devoted to the search for stoichiometric systems in which such insertions can be directly observed and investigated. Watson has reported[5a] the formation of an isobutyl complex from the insertion of propylene into the Lu–CH_3 bond of $(C_5Me_5)_2LuCH_3$; Stone,[7] Alt,[8] and Bergman and co-workers[9-11] have reported the formation of vinyl complexes from the insertion of unactivated[12,13] acetylenes into metal–carbon σ bonds.

Many of the catalytic reactions cited above involve planar complexes of d^8 metals such as Pd(II) and Pt(II). Although the direct observation (uncomplicated by subsequent reactions) of the insertion of a free olefin or unactivated acetylene into a Pd–C or Pt–C bond has not been reported,[14] the insertion of olefins and acetylenes into Pd–H and Pt–H bonds have been extensively studied.[15,16] Thorn and Hoffmann have carried out a detailed

(1) Maitlis, P. M. *Acc. Chem. Res.* **1976**, *9*, 93.
(2) Vollhardt, K. P. C. *Acc. Chem. Res.* **1977**, *10*, 1.
(3) Mullen, A. In "New Syntheses with Carbon Monoxide"; Falbe, J., Ed.; Springer-Verlag: New York, 1980; Chapter 3 and references therein.
(4) Heck, R. F. *Acc. Chem. Res.* **1979**, *12*, 146 and references therein.
(5) (a) Watson, P. L.; *J. Am. Chem. Soc.* **1982**, *104*, 337. Watson, P. L.; Roe, D. C. *J. Am. Chem. Soc.* **1982**, *104*, 6471 and references therein. (b) Soto, J.; Steigerwald, M. L.; Grubbs, R. H. *J. Am. Chem. Soc.* **1982**, *104*, 4479 and references therein.
(6) (a) Ivin, R. J.; Rooney, J. J.; Stewart, C. D.; Green, M. L. H.; Mahtab, R. *J. Chem. Soc., Chem. Commun.* **1978**, 604. (b) Turner, H. W.; Schrock, R. R.; Fellmann, J. D.; Holmes, S. J. *J. Am. Chem. Soc.* **1983**, *105*, 4942 and references therein.
(7) Davidson, J. L.; Green, M.; Nyathi, J. Z.; Scott, C.; Stone, F. G. A.; Welch, A. J.; Woodward, P. *J. Chem. Soc., Chem. Commun.* **1976**, 714.
(8) Alt, H. G. *J. Organomet. Chem.* **1977**, *127*, 349. Alt, H. G.; Schwarzle, J. A. *Ibid.* **1978**, *155*, C65. Alt, H. G. *Z. Naturforsch., B: Anorg. Chem. Org. Chem.* **1977**, *32B*, 1139.
(9) Tremont, S. J.; Bergman, R. G. *J. Organomet. Chem.* **1977**, *140*, C12.
(10) Huggins, J. M.; Bergman, R. G. *J. Am. Chem. Soc.* **1981**, *103*, 3002.
(11) Watson, P. L.; Bergman, R. G. *J. Am. Chem. Soc.* **1979**, *101*, 2055.
(12) As has been pointed out previously,[10] considerably more examples are known where the acetylene is activated by aryl, fluoro, carboalkoxy, or other electron-withdrawing substituents. Some of these examples are listed in ref 13.
(13) (a) Clark, H. C.; Jablonski, C. R.; von Werner, K. *J. Organomet. Chem.* **1974**, *82*, C51. (b) Clark, H. C.; Puddephatt, R. J. *Inorg. Chem.* **1970**, *9*, 2670. (c) Clark, H. C.; von Werner, K. *J. Organomet. Chem.* **1975**, *101*, 347. (d) Davies, B. W.; Payne, N. C. *J. Organomet. Chem.* **1975**, *102*, 245.
(14) Examples involving Ni–C bonds are reported in ref 9 and 10.

0002-7863/84/1506-5505$01.50/0